International Journal of Thin Films Science and Technology

http://dx.doi.org/10.18576/ijtfst/130312

New Configuration of Solar Cells Based on Perovskites Active Materials

Zainab R. Abdulsada[1,] and Ahmed A. Sharrad[2].*

[1] Department of Physics, College of Science, University of Thi –Qar, Thi-Qar, Iraq.
[2] General Directorate of Education in Muthanna, Iraq.

Received: 12 Jul. 2024, Revised: 12 Aug. 2024, Accepted: 22 Aug. 2024
Published online: 1 Sep. 2024

Abstract: In this paper, the focus was on organic and inorganic perovskite solar cells because of their exceptional light-harvesting capabilities, high efficiency, low production costs, and superiority over conventional solar cell materials. The findings demonstrated that, in contrast to solar cells based on lead, such those made of lead perovskite CH3NH3PbI3, Higher temperatures have less of an impact on lead-free sub-perovskite cells' outstanding performance. Lead-free perovskite solar cells have recently achieved high efficiencies of about 18.79 percent. A perovskite-based planar heterogeneous solar cell's conventional design consists of a transparent electrode, a back electrode, a hole transfer material (HTM), and a perovskite absorber together with electron transfer material (ETM). In this research, ETM (SnO_2) with perovskite $CH_3NH_3PbI_3$ and Spiro-Cu_2O as (HTM)/was used. This compound achieved a high efficiency of 18.79%. Method/Analysis: The Solar Cell Power Simulator (SCAPS) is used to evaluate the solar cell design.

Keywords: Perovskites materials, solar cells power simulator, solar cells, bandgap energy, photovoltaic (PV), back contacts.

1 Introduction

Over the past several decades, there has been a tremendous advancement in solar photovoltaic technology due to advancements in technology, research into novel, inexpensive materials, and increased commercial manufacturing. To get this technology on the market, solar cell efficiency must be increased as much as feasible. The energy loss caused by the gap is one of the single-junction photovoltaic (PV) devices' limitations. Between the photon energy and the material's (Eg). It is well known that photon energy must match the bandgap energy to be successfully extracted as electric power. Photon energy is simply not absorbed when it is less than the bandgap energy, Moreover, when it surpasses the bandgap energy, carrier thermalization causes the excess energy to be wasted, which hinders the conduction process [1]. This cell is manufactured by directly depositing layers one on top of the other new perovskite families or III-V semiconductor compounds can be used to create this kind of cell.

The lengthy diffusion length and significant optical absorption [2], charge carrier mobility [3], and wide tunable (Eg) (between from 1.48 to 2.23 V) of perovskite materials have also been shown to be extremely promising [4]. A perovskite compound made of metal halides is used as a light absorber in perovskite solar cells. Perovskite molecules, the building blocks of a photovoltaic solar cell, contain the general chemical formula ABX3, where X is an anion and A and B are cations with different atomic radii (A is bigger than B). Organic-inorganic hybrid metal halide perovskites have a crystal structure similar to that of calcium titanium oxide (CaTiO3) [5].

2 Methodology

The system is predicated on carrying out three fundamental actions for every layer. The thickness, temperature, and gap energy (Eg) are measured in the first stage at intervals of [Range from 213 k to 300 k].

Information on these four attributes, which include efficiency(η), Voc, Jsc, and FF, will be gathered. SCAPS-1D software was used to obtain these results, the main goal of SCAPS-1D is to resolve the Poisson and continuity equations [6][7]. Any equation begins at the beginning of this period and starts with the basic assumption that a balance is achieved by using the quasi-Fermi level. In this instance, no illumination nor voltage are added.

The ratio between the generated maximum power and the incident power is used to calculate power conversion efficiency.

This is given by:

$$\eta = \frac{P_{max}}{p_{in}} = \frac{J_{SC}V_{OC}FF}{P_{in}} \quad (1)$$

The parameters of each layer are determined here according to the table below

*Corresponding author E-mail: zainab_rah.ph@utq.edu.iq

Table 1: The materials parameters numerical analysis [8-11]

Parameters	Sipro-OMeTAD	Cu2O	$MAPbI_3$	Sno2
Band gap(ev)	3.2	2.17	1.55	3.6
Electron effinity (ev)	2.1	3.2	3.75	4
Dielectric permittivity	3	7.11	6.5	9
CB effective density of states (1/cm2)	2.50E+18	2.02E+17	2.20E+13	2.200E + 18
VB effective density of states (1/cm2)	1.80E+19	1.10E+19	2.20E+12	1.800E + 19
Electron thermal velocity(cm/s)	1.00E+07	1.00E+07	1.00E+07	1.000E + 7
Hole thermal velocity(cm/s)	1.00E+07	1.00E+07	1.00E+07	1.000E + 7
Electron mobility (cm2/v.s)	2.00E-04	2.00E+02	2.00E+00	1.000E + 2
Hole mobility (cm2/v.s)	2.00E-04	8.00E+18	2.00E+00	2.500E + 1

3 Result and Discussion

3.1. Effect layer thickness of (n ITO/SNO2/CH3NH3Pb I3/CU2O/AU (p)

In order to produce electron-hole pairs and absorb the greatest number of photons, the absorber layer should be adjusted to its ideal thickness [12]. The thickness of the absorber layer has been adjusted from 0.01µm to 0.14µm.

Efficiency, Voc, Jsc, and F.F. drop as the absorber layer thickness rises because the production of electron-hole pairs in the perovskite materials reduces as thickness increases. The maximum efficiency at the thickness 0.01 the efficiency is 18.70%.

Table 2: Variation of Thickness for ITO/SNO2/CH3NH3Pb I3/CU2O/AU with solar cells parameters.

Thickness (µm)	Voc (V)	Jsc (ma/cm2)	F.F (%)	η (%)
SNO2				
0.01	0.786	40.62	58.53	18.7
0.02	0.786	40.54	58.49	18.65
0.03	0.7863	40.44	58.46	18.59
0.04	0.7862	40.35	58.43	18.54
0.05	0.7861	40.26	58.41	18.49
0.06	0.7861	40.18	58.39	18.44
0.07	0.786	40.11	58.37	18.4
0.08	0.7859	40.05	58.35	18.37
0.09	0.7859	40	58.34	18.34
0.1	0.7859	39.96	58.32	18.32
0.11	0.7858	39.92	58.31	18.29
0.12	0.7858	39.88	58.3	18.27
0.13	0.7858	39.85	58.29	18.26
0.14	0.7858	39.83	58.29	18.24

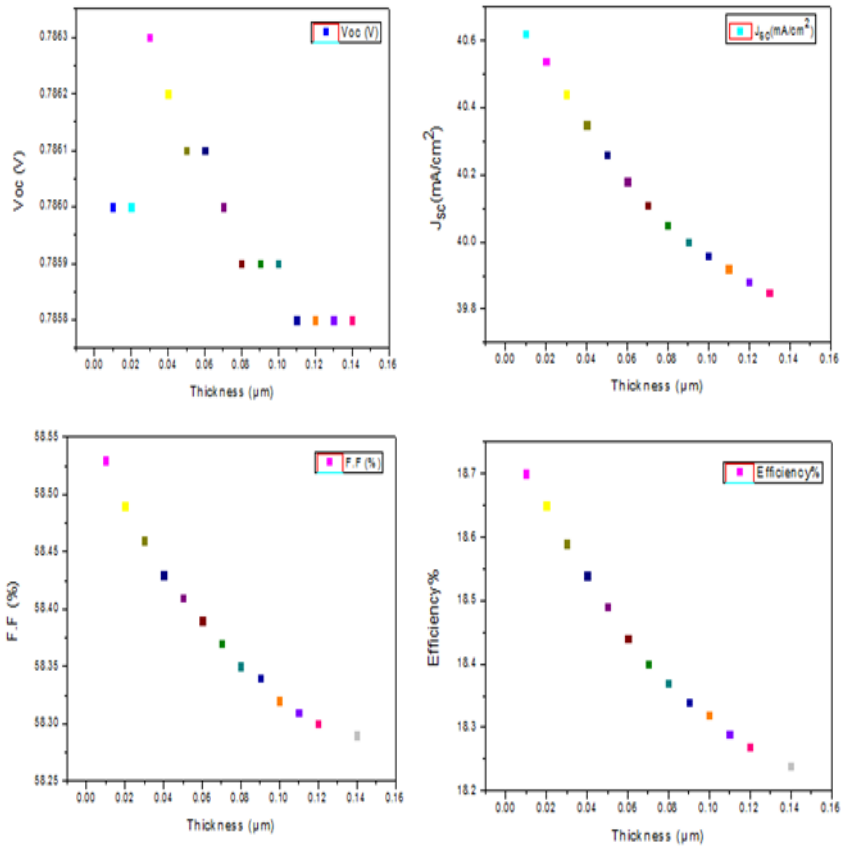

Fig. 1: PV parameter variation via altering the thickness of ITO/SNO2/CH3NH3Pb I3/CU2O/Au.

3.2. Effect of annealing Temperatures for ITO/SNO2/CH3NH3Pb I3/CU2O/AU

Table 3 displays the simulation's findings for I-V characteristics, including PCE, FF, Jsc, and Voc, for a PVSC across a range of environmental temperatures. The maximum efficiency is 18.79% with Jsc = 40.32mA/cm2, FF = 61.79% and Voc = 0.73volt is attained when the temperature reaches 333 K, making the optimal outcome at extremely low temperatures ideal for operations in space. As seen in Fig. 2, the PCE, F.F., and Jsc increase as the temperature rises from 213 K to 333 K. According to Fig. 2, open-circuit voltage typically drops progressively as temperature rises, due to its ability to regulate charge carrier production, recombination, and collection, temperature can alter efficiency. As a result, the optimal temperature of a PVSC using SNO2 as a PVSC is 333 k.

Table 3: The parameter of ITO/SNO2/CH3NH3Pb I3/CU2O/AU heterojunction solar cells

T(K)	Voc (V)	Jsc (mA/cm2)	F.F (%)	η (%)
213	0.91	40.19	46.2	16.91
233	0.88	40.37	48.5	17.28
253	0.85	40.55	51.03	17.67
273	0.82	40.74	53.74	18.06
293	0.79	40.94	56.58	18.43
313	0.79	40.94	56.58	18.43
333	0.73	40.32	61.79	18.79

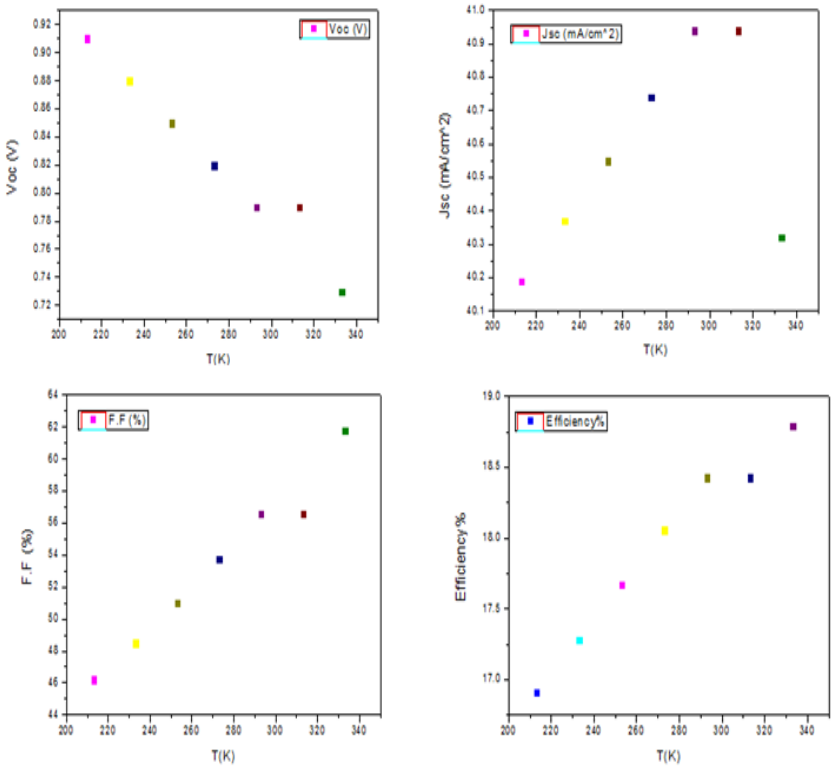

Fig. 2: The relationship between temperature and solar cell characteristics.

3.3. The impact of various back contacts acting as electrodes

Utilizing simulations, Chromium (Cr), silicon (Si), silver (Ag), titanium (Ta), nickel and (Zn) as a potential back contact for photovoltaic solar cells. Figure 3 illustrates the impact of the back contacts' varying performances. The Voc, Jsc, and FF rise as the metal is more useful. As a result, PVSC efficiency is also rising. Due to the electrical field becoming negative at the HTM and back contact [13], the holes cannot move toward the electrode because of energy disfavor. Ta is among the possible back contact materials that might improve PSC performance, according to the simulation's findings.

Table 4: demonstrates how different metal back contacts affect different HTM layer candidates.

Efficiency%	F.F (%)	$J_{sc}\,(mA/cm^2)$	$V_{oc}\,(V)$	Work Function (ev)	Metals
15.42	49.4	25.79705	1.2103	4.5	Cr
17.21	51.58	26.10516	1.2782	4.6	Si
18.13	53.83	26.26226	1.2826	4.7	Ag
18.23	54.06	26.28	1.2828	4.8	Ta
18.23	54.07	26.28079	1.2828	4.9	Zn

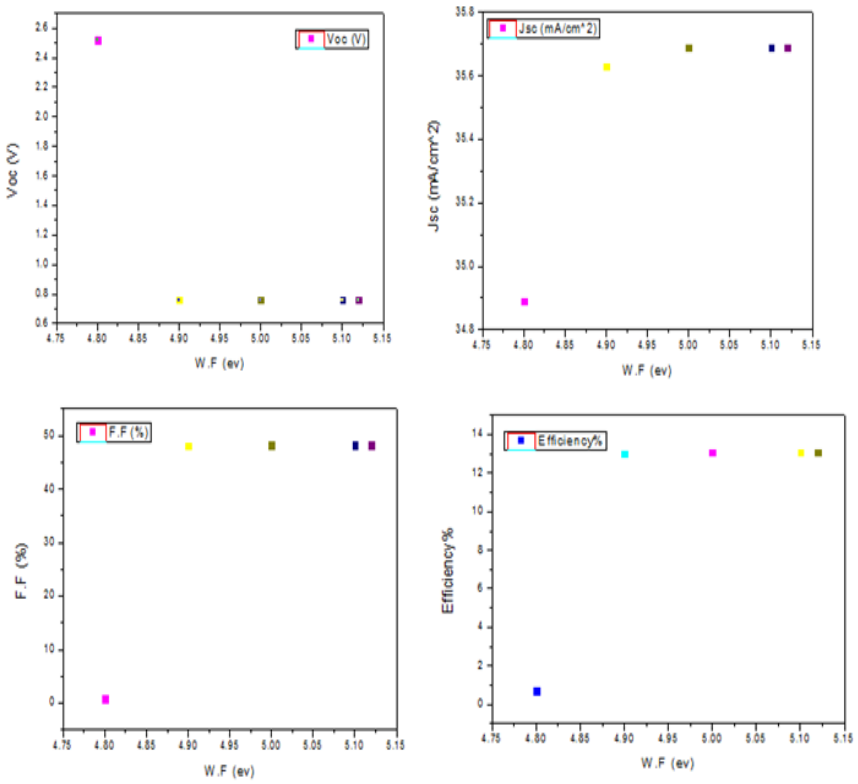

Fig. 3: The relationship between Metalwork function and solar cell characteristics

4 Conclusions

The thickness of CH3NH3Pb I3 was varied in this study in order to observe each substance. Additionally, a range of temperatures and work functions were investigated in order to determine the ideal conditions that corresponded to the highest efficiency of the material such as SNO2/CH3NH3Pb I3/CU2O, have been designed which are utilized as ETL, HTL and buffer layers in perovskite solar cells to accomplish high PCE and stability, which was 18.79%.

Acknowledgments

We are grateful to Samir M. AbdulAlmohsin Thi Qar University, our supervisor, and Mark Burger Man of the University of Gent, Belgium's Electronic and Information System (Elis) for granting us free access to the Scaps simulation program.

References

[1] Miller, O.D.; Yablonovitch, E. (2021). Photon extraction: The key physics for approaching solar cell efficiency limits. Act Photonic Mater V [Internet]. International Society for Optics and Photonics. Available online: https://www.spiedigitallibrary.org/conferenceproceedings-of-spie/8808/880807/Photon-extraction--the-key-physics-for-approaching-solar-cell/10.1117/12.2024592.short (accessed on 1 June 2021).

[2] Stranks, S.D.; Eperon, G.E.; Grancini, G. (2014). Electron-Hole Diffusion Lengths Exceeding 1 Micrometer in an Organometal Trihalide Perovskite Absorber. *Science* **2013**. [CrossRef]

[3] Ponseca, C.S.; Savenijie, T.J.; Abdellah, M. Organometal Halide Perovskite Solar Cell Materials Rationalized: Ultrafast Charge Generation, High and Microsecond-Long Balanced Mobilities, and Slow Recombination. *J. Am. Chem. Soc.* **2014**. [CrossRef]

[4] Zhu, S.; Yao, X.; Ren, Q.; Zheng, C.; Li, S.; Tong, Y.; Shi, B.; Guo, S.; Fan, L.; Ren, H.; et al. Transparent electrode for monolithic perovskite/silicon-heterojunction two-terminal tandem solar cells. *Nano Energy* **2018**, *45*, 280–286. [CrossRef]

[5] Yang Yang, ... Hongxia Wang. (2022). " Perovskite solar cells based self-charging power packs: Fundamentals, applications and challenges", in Nano Energy,

[6] Dhuha E. Tareq, Samir M. AbdulAlmohsin, Hussein H. Waried. (2020). "High Efficiency (41.85) of Br Perovskites base solar cells with ZnO and TiO2 comparable study as ETM" , IOP Conference Series: Materials Science and Engineering,

[7] M. A. Halim, S. K. Biswas, M. S. Islam, and M. M.

Ahmed, (2022). “Numerical simulation of non-toxic ZnSe bufer layer toenhance Sb2S3 solar cell efciency using SCAPS-1D soft-ware,” International Journal of Robotics and Control Systems,vol. 2, no. 4, pp. 709–720, 2022.

[8] Zainab. R. Abdulsada, Samir M . AbdulAlmohsin . (2021). “High Efficiency Solar Cells Base on Organic-inorganic Perovskites Materials”, University of Thi-Qar Journal of Science

[9] K. Sobayel, K. S. Rahman, M. R. Karim et al., (2018). “Numericalmodeling on prospective bufer layers for tungsten di-sulfde(WS 2) solar cells by SCAPS-1D,” Chalcogenide Letters,vol. 15, no. 6, 2018.

[10] D. I. Kim, J. W. Lee, R. H. Jeong, and J. H. Boo, “A high-efciency and stable perovskite solar cell fabricated in ambientair using a polyaniline passivation layer,” Scientifc Reports,vol. 12, no. 1, p. 697, 2022

[11] Zainab R. Abdulsada, Samir M. Abdul Almohsin. (2021). "High Efficiency (9.60) of CI Perovskites base solar cells with PCBM

[12] J. Tian et al., (2012). “Enhanced performance of CdS/CdSe quantum dot cosensitized solar cells via homogeneous distribution of quantum dots in TiO2 film,” J. Phys. Chem. C, vol. 116, no. 35, pp. 18655–18662, 2012.

[13] F. Behrouznejad, S. Shahbazi, N. Taghavinia, H.-P. Wu, and E. W.-G. Diau, (2016). “A study on utilizing different metals as the back contact of CH3NH3PbI3 perovskite solar cells,” Journal of Materials Chemistry A, vol. 4, pp. 13488–13498, 2016